

Polymer Membrane Formation through the Thermal-Inversion Process. 1. Experimental Study of Membrane Structure Formation

Gerard T. Caneba* and David S. Soong

Department of Chemical Engineering, University of California, Berkeley, California 94720.
Received April 11, 1985

ABSTRACT: Anisotropic polymer membranes have been successfully obtained via the thermal-inversion process. In contrast to conventional casting procedures by phase inversion, this process is less complicated but more flexible. In addition, the thermal-inversion process yields reproducible membranes with high porosities. In this work, conditions are delineated for the formation of anisotropic membranes on the basis of kinetic and thermodynamic considerations. Experimental findings verify these theoretical predictions for a particular polymer/solvent pair. Finally, asymmetric membranes with graded pore size profiles and a thin dense working skin can be obtained from a variation of the basic thermal-inversion procedure.

Introduction

Since their discovery in the early 1960s,¹ anisotropic polymer membranes have been prepared solely through the phase-inversion process. Here, a thin coating (100–300 μm) of a polymer solution (e.g., cellulose acetate in acetone) is first spread on a solid support. The coated surface is then coagulated with a nonsolvent (e.g., water); this process is followed by annealing of the resulting membrane in a warm nonsolvent bath. Final structures range from having isotropic, dense or porous, cross sections to those with graded pore size profiles, with or without thin dense skin layers on either or both surfaces. Tanny² classified membranes with graded pore size profiles as anisotropic membranes, while porous and anisotropic membranes with thin skin layers were called asymmetric membranes. Normally, asymmetric membranes with graded pore size profiles have skin layers adjacent to the side of the membrane with smaller pores. In this work, we will refer to this specific type as anisotropic asymmetric membranes, i.e., skinned membranes with an internal pore size gradient.

Membrane formation through the phase-inversion casting procedure involves a combination of complicated transport and thermodynamic phenomena.³ During coagulation, nonsolvent penetrates into the polymer coating, while solvent diffuses out into the nonsolvent. (See Figure 1). Regions depleted of the solvent and penetrated by the nonsolvent begin to phase separate, since the local compositions correspond to points inside the two-phase envelope of the particular polymer/solvent/nonsolvent ternary diagram. With the use of trajectories for the global average compositions of the coagulating membrane on a phase diagram, Strathmann, Scheible, and Baker⁴ delineated certain rules of thumb for obtaining dense, porous, or asymmetric membrane products (Figure 2). When the trajectory is close to the polymer-rich side of the phase envelope, the resulting membrane is a dense one. In contrast, with a trajectory close to the dilute polymer phase, a porous structure results. Asymmetric membranes are obtained for cases with a trajectory between these two.

A new membrane casting method can be envisioned where temperature reduction rather than the nonsolvent serves the role of the coagulant (Figure 3). Structure formation is carefully induced and completed by a programmed sudden cooling of one face of the polymer solution, whereby phase separation is initiated. This phase-separation process propagates gradually inward as the

temperature of successive fluid layers drops from the continual heat removal. Incipient phase-separated morphology is not only formed but also perfected at different temperatures in different layers of the membrane. Such a casting strategy, if capable of yielding a wide variation of membrane structure, may allow better process control and reproducibility.⁵ In addition, the time-dependent temperature profile and propagation of the phase-separation front can be independently fine-tuned to permit greater process flexibility. The details of this proposed binary casting procedure are amenable to mathematical modeling and systematic experimental investigation.

Porous membranes with and without thin skin layers (around 0.5 μm) on one or even both sides have already been obtained previously by a binary casting process (called thermal-inversion, thermal-coagulation, or thermal-casting process).^{2,6,7} Castro⁵ reported the following advantages of the thermal-casting process: (a) high void volumes obtained from product membranes (about 80%) with pore sizes ranging from 0.1 to 5 μm and (b) better process control compared with the phase-inversion process. Commercial thermal-cast polypropylene membranes are manufactured by Hydronautics and Membrana, Inc.⁷

In this work, we ascertain the feasibility of a modified thermal casting procedure and determine its appropriate conditions to produce anisotropic polymer membranes. Detailed experimental observations and their theoretical interpretations will be reported here. An extensive modeling effort will, however, be deferred to part 2 of this series.

Theory

Liquid-Liquid Phase-Separation Mechanism. According to Broens et al.,³ nucleation and growth and spinodal decomposition are two possible phase-separation mechanisms that can occur in a phase-inversion casting process. If a trajectory (in a binary phase diagram) representing an infinitesimal slice (perpendicular to the thickness direction) of the membrane during coagulation is followed closely, it can be noted that the trajectory first passes through the metastable region before reaching the unstable region (Figure 4). For a noncrystalline polymer, we consider spinodal decomposition as the more likely phase-separation mechanism. Typically, starting cast solution compositions are close to the critical composition of the binary phase diagram; thus, during coagulation, different parts of the membrane spend very little time inside the metastable region. With the use of a noncrystallizable polymer, we assume that homogeneous nucleation does not occur during the time when different parts

* Present address: Department of Chemistry and Chemical Engineering, Michigan Technological University, Houghton, MI 49931.

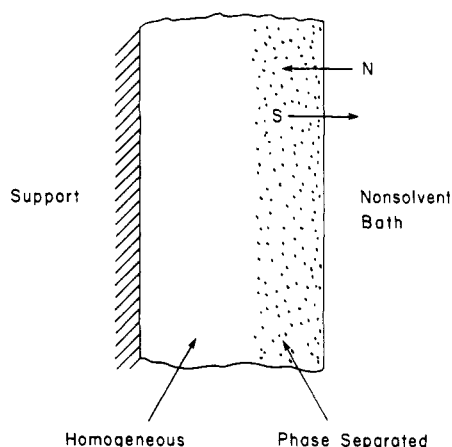


Figure 1. Schematic diagram of the formation of structured polymer membranes through the phase-inversion process. The phase-separation front propagates from the face exposed to the nonsolvent coagulant bath, which provides the nonsolvent penetrant and extracts the solvent from the original casting solution.

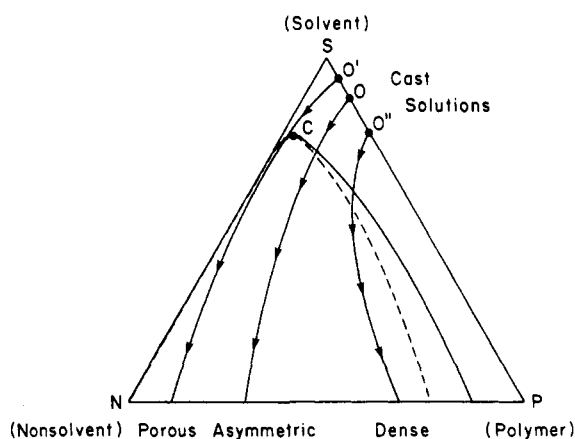


Figure 2. Trajectories of overall composition of membrane during phase-inversion coagulation. Different initial solution concentrations lead to varying final membrane structures, depending on the thermodynamic and kinetic characteristics of the ternary system.

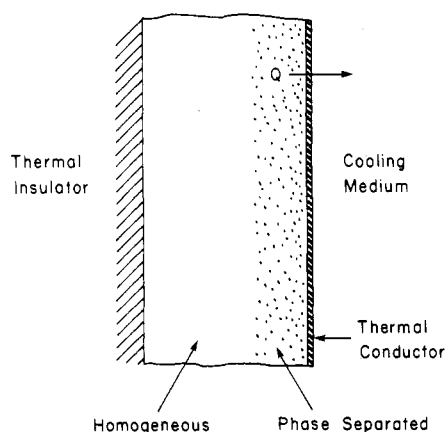


Figure 3. Schematic diagram of the formation of structured polymer membranes through the thermal casting process. Heat is removed through the thin conducting surface, whereby phase separation is initiated, while the backside temperature is protected by the insulating substrate.

of the membrane are in the metastable region.

Evolution of Structure during Phase Separation.

When the temperature of a binary polymer/solvent system is quickly reduced from above the critical point into the phase-separated region, a number of observations have been noted based on our mathematical modeling work.

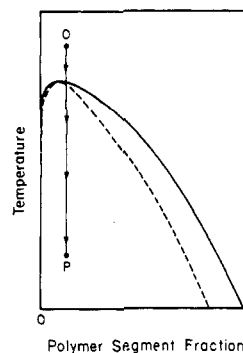


Figure 4. Typical trajectory of overall composition of membrane during thermal coagulation. The starting solution at point O is homogeneous. A lower temperature (point P) is suddenly applied to one face of the membrane where phase separation is initiated.

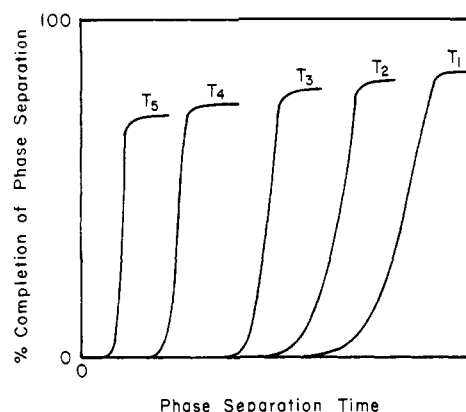


Figure 5. Percentage completion curves for phase separation induced by a step reduction in temperature from the initial state to different final temperatures ($T_1 > T_2 > T_3 > T_4 > T_5$).

Figure 5 shows that structural growth is relatively abrupt; i.e., the bulk of the growth occurs in a short period of accelerated structure formation. This result implies that the phase-separated front in the coagulating membrane is rather sharp. For membrane formation through the phase-inversion process, this phenomenon, although not yet pointed out specifically, can be observed in the works of a number of investigators.⁸⁻¹¹ Figure 5 also reveals the systematic variation in the induction periods with the prevailing phase-separation temperature. Note that at about 40% completion of the phase-separation process during the growth period, the final pore size no longer changes when the temperature is lowered further; i.e., the original structure is locked in. The different phase-separation temperatures in the induction periods can therefore explain anisotropies obtained in the final structures of thermal-cast membranes. The infinitesimal slice of membrane material near the cooling medium is exposed to a cooler temperature than a slice near the thermal insulator backing. The former slice thus reaches its growth phase at a lower temperature than the latter slice. As a consequence, the material slice close to the cooling medium effectively phase separates at a lower temperature than the material close to the thermal insulator.

Effects of Transport and Thermodynamic Parameters on Structure Formation. Even though the detailed model will be reported in part 2 of this series, we will summarize its major findings here to aid the discussions of the experimental observations.

Perhaps the most relevant results of our modeling work are (a) the induction period for the formation of structure decreases with an increase in the magnitude of the mutual diffusivity at the average concentration of the system and

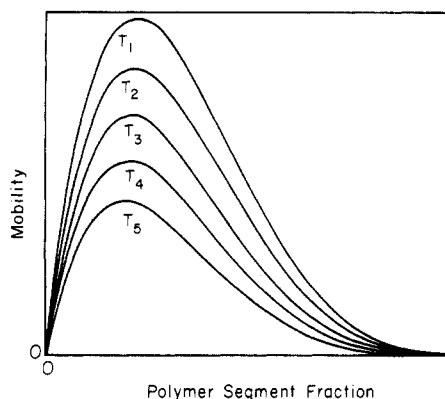


Figure 6. Temperature and concentration dependence of the mobility factor for a binary polymer solution covering the phase-separated region ($T_1 > T_2 > T_3 > T_4 > T_5$).

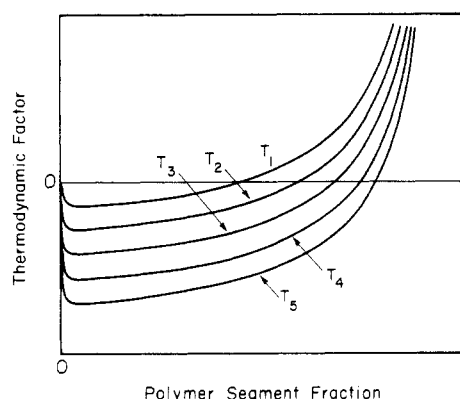


Figure 7. Temperature and concentration dependence of the thermodynamic factor for a typical polymer/solvent system covering the phase-separated region ($T_1 > T_2 > T_3 > T_4 > T_5$).

(b) the final pore size decreases with an increase in the magnitude of the thermodynamic factor of the polymer/solvent system. (The mutual diffusivity is equal to the product of the mobility and the thermodynamic factor.)¹² For polymer solutions undergoing phase separation, the mobility and mutual diffusivity are both strong functions of concentration and temperature.¹²⁻¹⁵ We will therefore separately analyze the mobility factor and thermodynamic factor and then deduce the dependence of the mutual diffusivity on concentration and temperature.

Using the free-volume concepts for the self-diffusivities of the polymer and solvent¹²⁻¹⁵ and an expression for the mobility factor adopted from Cahn and Hilliard¹⁶ and Vrentas and Duda,^{12,13} we predicted the family of mobility vs. concentration curves in Figure 6. Note that the mobility is always positive, and it exhibits a relative maximum with concentration. In addition, the mobility at a given polymer concentration increases with temperature. For the thermodynamic factor (Figure 7), we used the Flory-Huggins expression for the Gibbs energy of mixing¹⁷ with the χ -parameter composed of an entropic and an enthalpic part.¹⁸ Both the entropic and enthalpic contributions to the χ -parameter are assumed to be independent of concentration. The entropic term is independent of temperature, whereas the enthalpic part is inversely proportional to the temperature. With these assumptions, the calculated value of the thermodynamic factor at a given concentration increases with temperature. (Note that for concentrations inside the spinodal region the thermodynamic factor is negative.) In addition, the larger enthalpic contributions to the χ -parameter give greater variations of the thermodynamic factor with temperature. This corresponds to a system with a large energy of interaction

Table I
Actual Concentrations of Cast Solutions Obtained from ¹³C FTNMR Spectroscopy

nominal wt % polymer	actual wt % polymer
5	4.8 ± 0.5
10	9.7 ± 0.4
15	14.5 ± 0.2

between the components,¹⁸ as is often realized for highly polar polymer-solvent pairs. For nonpolar systems there is not much change of the thermodynamic factor with temperature; temperature variation in mutual diffusivity is primarily caused by the mobility factor.

We identify two temperature effects governing the formation of anisotropic membranes: zeroth-order and first-order effects. Zeroth-order effect relates to the pore size obtained as a function of coagulation temperature. Hence, the thermodynamic factor imparts a zeroth-order effect to the casting process. The first-order effect is attributed to the temperature history experienced by a given slice of material in the membrane. This would then be related to the induction time for phase separation begun at a particular temperature. On the basis of on the above discussion, we conclude that differences in the mutual diffusivities cause varying first-order effects on membrane formation. Thus, the thermodynamic aspect of phase separation is responsible for the range of possible pore sizes in thermal-cast membranes, whereas the heat and mass transport aspects of phase separation determine the distribution of pore sizes.

Experimental Section

Preparation and Characterization of Cast Solutions. Reagent-grade (MW >100 000) atactic poly(methyl methacrylate) (PMMA), purchased from Aldrich Chemical Co., was used in this study. This polymer was chosen partly because it does not form crystallites. Crystal formation would complicate our subsequent modeling work. Sulfolane (tetramethylene sulfone or 1,1-tetrahydrothiophene dioxide), a liquid that solidifies at 27 °C, was used as the solvent. Such a solidification point is convenient for freezing pore structures of coagulated membranes. Solutions of about 5%, 10%, and 15% PMMA (w/w) in sulfolane were prepared. Particulate contaminants were removed through high-temperature vacuum filtration. Actual concentrations of the final cast solutions were then obtained by using the FTNMR techniques described below (Table I).

Determination of Binary Phase Diagram. The binary phase diagram was obtained with techniques described elsewhere.¹⁹ Only one sample (with composition close to the critical point) was needed to perform this series of experiments. In this case, the sample was about 15% (w/w) PMMA in sulfolane. Since a tie line corresponds to one temperature, ¹³C FTNMR spin-lattice relaxation experiments were performed at different temperatures. To ensure that the sample was at thermodynamic equilibrium, it was first heated to a temperature above the critical temperature of the binary system for at least 1 day. The sample was then immersed in a water bath maintained at a temperature where the phases separated. Before the sample was used for a relaxation experiment, it was kept in the water bath for at least 1 day to ensure complete phase separation. Longer periods of holding times (up to 1 week) were employed at lower temperatures. Although the phase diagram obtained by analyzing spin-lattice relaxation data was only exact for reasonably monodisperse polymer (the PMMA sample used has a polydispersity index greater than 2.0), the plot served as a useful guide in designing detailed membrane preparation procedures.

Thermal Casting Apparatus and Procedure. Figure 8 shows a schematic of the casting cell used in making thermal-cast membranes. The starting polymer solution is confined within a thin aluminum sheet (0.01 in. thick) and Teflon block (1 in. thick and 5 in. in diameter) and template (200–500 μm thick). The Teflon pieces are used because they are good thermal insulators. The thin metal sheet is used to ensure that the polymer solution

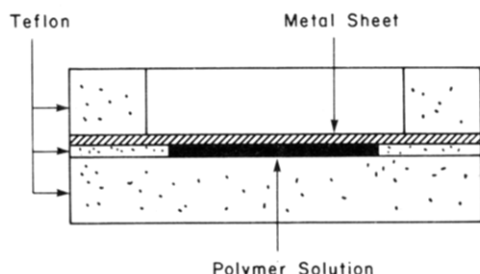


Figure 8. Schematic diagram of the casting cell used for thermal inversion of PMMA membranes.

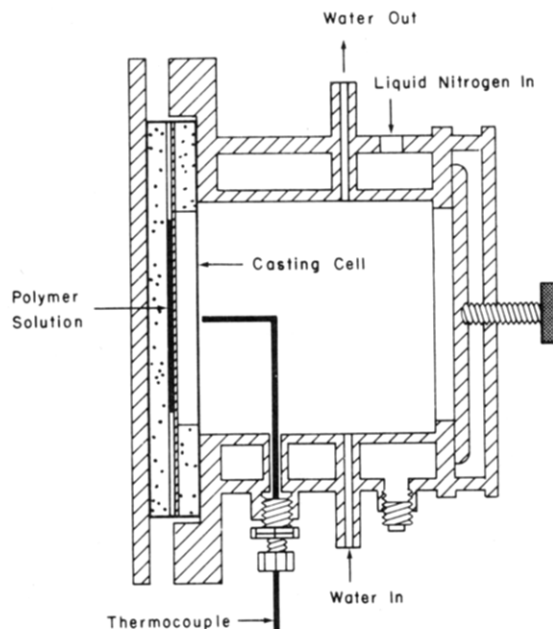


Figure 9. Schematic diagram of the casting cell assembly used to expose the casting cell to different temperatures.

in contact with the metal is in rapid thermal equilibrium with the instantaneous temperature on the other side of the metal plate. To avoid leakage of the polymer solution, the Teflon block and metal sheet sandwiching the thin Teflon template are tightly clamped with bolts.

The casting cell is held inside the cell assembly (Figure 9). Fluid used to thermally equilibrate the polymer solution is allowed to circulate inside the casting cell. For our system, we used water at the specified coagulating temperature for the binary mixture. To apply a higher temperature to the polymer solution inside the casting cell, the front of the assembly can be taken out and hot air blown through the opening. For subambient temperatures, ambient air is blown through the opening in front of the assembly, while liquid nitrogen is introduced into the annular space at the side of the assembly.

Before the polymer solution was poured into the cell, it was heated (to about 80 °C) and stirred in its container for at least an hour. This was done to ensure that the starting solution was homogeneous. After the solution was poured into the casting cell, it was mounted inside the casting cell assembly. Air at about 80 °C was blown continuously through the cell for about 15 min. This temperature is sufficiently above the critical temperature of our binary mixture. To phase separate the solution, the opening in front of the casting cell assembly was closed off and water at the coagulating temperature was run through the assembly for at least 30 min. Finally, to freeze the polymer structure of the coagulated mixture, the front of the casting cell assembly was again opened and air was blown through the opening while liquid nitrogen was poured into the annular part of the assembly. The temperature of the system was then lowered to about 0 °C (i.e., below the freezing point of the solvent) for about 15 min. The cell was then opened, and the membrane was immersed in water at room temperature to allow the solvent to leach out. This final step did

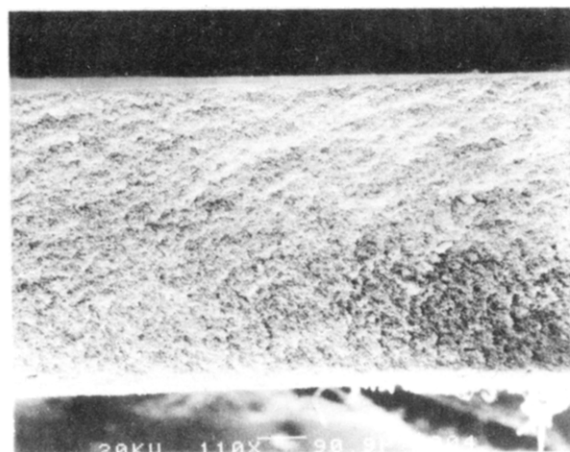


Figure 10. Scanning electron micrograph of a PMMA membrane cross section cast from a 10 wt % solution with the thermal casting procedure. Scale bar corresponds to 90.9 μm .

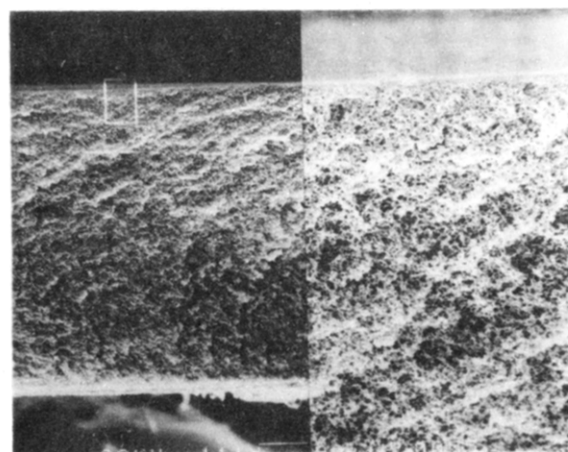


Figure 11. Scanning electron micrograph of a PMMA membrane cross section cast from a 10 wt % solution with the thermal casting procedure. An expanded view of the boxed section in the left frame is shown on the right. Scale bar corresponds to 90.9 μm .

not change the existing membrane pore structure, due to the presence of the nonsolvent, water, at the leaching temperature. Product membranes were stored in water for the following characterization work.

Scanning Electron Microscopy. For SEM studies, wet PMMA membranes were first freeze-dried at -6.5 °C. This low temperature ensured complete retention of the pore structures of the membranes during water removal. Freeze-drying porous membranes with an area of about 2 cm² and a thickness ranging from 200–500 μm took less than 2 h. For dense membranes, the drying time could take as long as 10 h. In order to expose their cross sections, the dried membranes were cracked in liquid nitrogen. The cracked pieces were then mounted on an SEM sample stage and subsequently coated with gold in a Polaron sputter coater. Finally, the coated samples were viewed (with magnifications ranging from 100 to 15 000 \times) and photographed with an ISI-DS-130 scanning electron microscope.

Results and Discussion

Figures 10–14 show scanning electron micrographs of a thermal-cast membrane from a starting PMMA/sulfolane solution of about 10 wt % PMMA. The full cross section, as seen in Figure 10, shows that the membrane does not have a uniform pore size. The top part, the portion adjacent to the cooling medium during casting, has smaller pores. The graded pore size profile exhibited by this membrane is clearly shown in Figure 11, where a small area of membrane cross section near the top is magnified. Figure 12 provides a close-up of the top surface of this

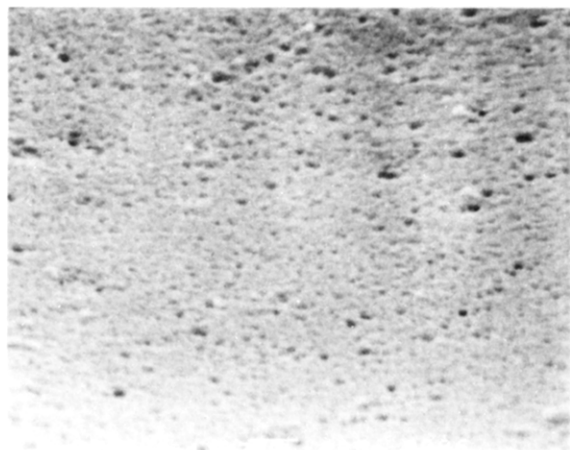


Figure 12. Scanning electron micrograph of the surface of the thermal-cast PMMA membrane in contact with the thin conducting material during coagulation. The starting solution is 10 wt % PMMA, and pores on this surface are 0.1–0.2 μm in diameter. Scale bar corresponds to 0.885 μm .

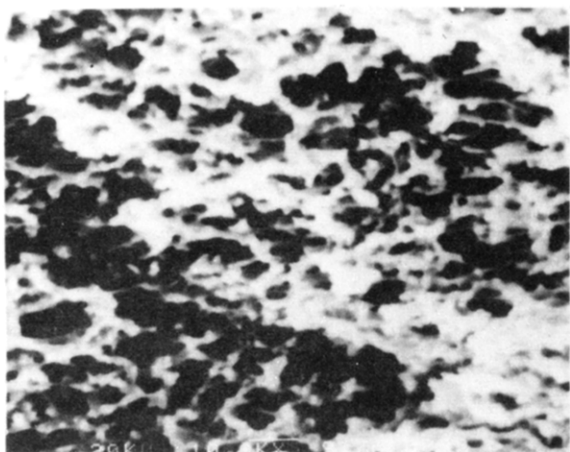


Figure 13. Scanning electron micrograph of the cross section of the middle portion of a thermal-cast PMMA membrane from 10 wt % solution showing 1- μm honeycombed cells bounded by 0.3–0.5- μm open pores. Scale bar corresponds to 0.917 μm .



Figure 14. Scanning electron micrograph of the surface of the thermal-cast PMMA membrane in contact with the thermal insulator. The starting solution is 10 wt % PMMA, and pores on this surface are 2–15 μm in diameter. Scale bar corresponds to 13.7 μm .

membrane, which shows pores of 0.1–0.2 μm . The center of the cross section (Figure 13) consists of 1- μm honeycombed cells bounded by 0.3–0.5- μm open pores. Finally, Figure 14 shows the bottom surface of the membrane with

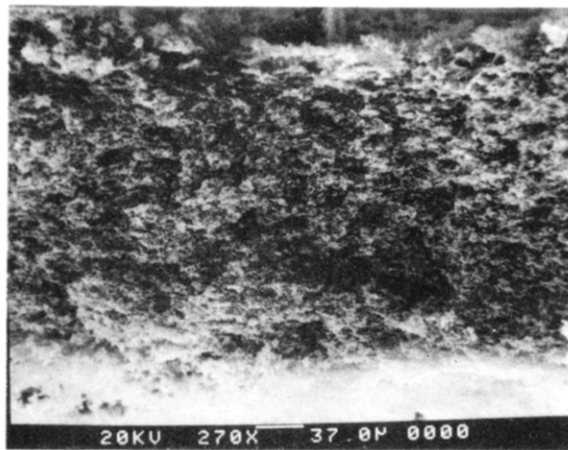


Figure 15. Scanning electron micrograph of the cross section of a thermal-cast PMMA membrane from 5 wt % solution. Scale bar corresponds to 37.0 μm .

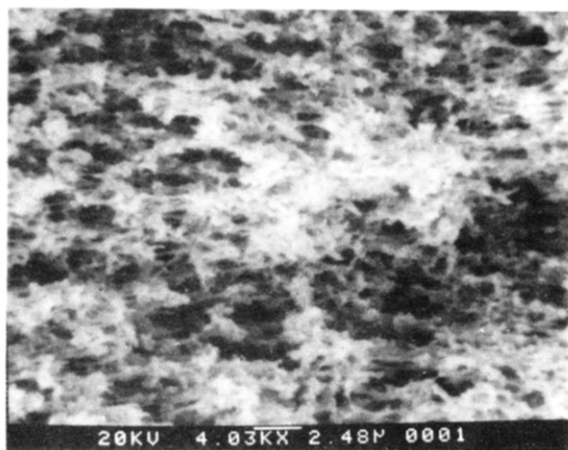


Figure 16. Scanning electron micrograph of the cross section of the middle portion of a thermal-cast membrane from 5 wt % solution showing 2- μm cells bounded by 1- μm open pores. Scale bar corresponds to 2.48 μm .

pores ranging from 2 to 15 μm . Therefore, from one face of the membrane to the other, the pore size gradually changes from 0.1–0.2 to 2–15 μm , and the membrane is distinctly anisotropic. Clearly, this sample is not asymmetric in the sense that a dense skin layer is not present on the top surface. The thermal casting process, however, can produce a dense top layer by the application of a quick high-temperature pulse on the side of the membrane in contact with the thermal conductor after the coagulation step. This short temperature pulse will cause a small portion of the top layer to dissolve. The structure is then frozen and the solvent leached out. Subsequent annealing of the product membrane will densify the top layer. Anisotropic asymmetric membranes can thus be made.

Figures 15 and 16 show SEM pictures of the membrane obtained from a starting solution of about 5 wt % PMMA in sulfolane. The membrane is seen to possess an isotropic porous structure. Note in Figure 16 that the pores of this membrane are of the same honeycombed, open structure as those obtained from a 10 wt % PMMA in sulfolane solution. Also, pore size is about 1 μm , while cell size is about 2 μm .

Figures 17–20 show SEM pictures of the PMMA membrane cast from 15 wt % PMMA in sulfolane. This membrane, like the one from the 10 wt % PMMA in sulfolane solution, exhibits a graded pore size profile. The only difference is that this membrane has smaller pores. The top layer, the portion of the membrane adjacent to

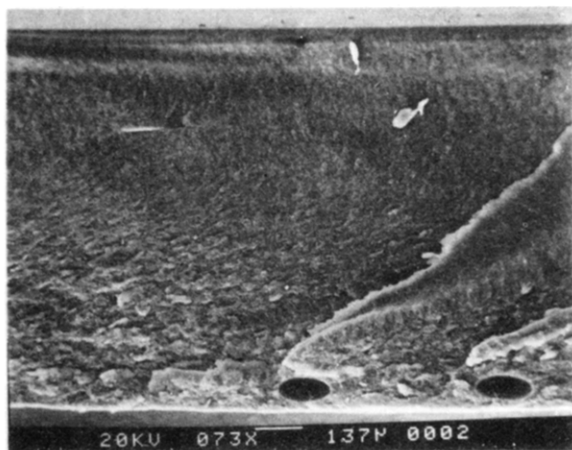


Figure 17. Scanning electron micrograph of the cross section of a thermal-cast PMMA membrane from 15 wt % solution. Scale bar corresponds to 137 μm .



Figure 18. Scanning electron micrograph of the surface and cross section of layer in contact with the thin conducting material for a thermal-cast PMMA membrane from 15 wt % solution. Pores on the top surface are less than 0.1 μm in diameter. Scale bar corresponds to 2.16 μm .

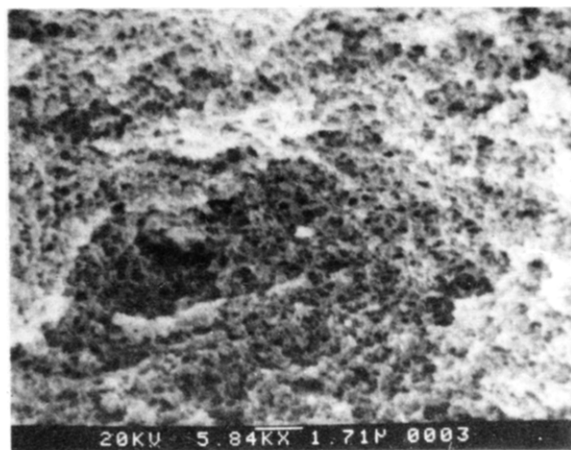


Figure 19. Scanning electron micrograph of the cross section of the middle portion of a thermal-cast PMMA membrane from 15 wt % solution showing 0.5- μm open pores. Scale bar corresponds to 1.71 μm .

the cooling medium, has a pore size less than 0.1 μm . The middle part of the cross section has 0.5- μm pores. Finally, the bottom part has about 1- μm pores.

Experimental observations of anisotropic membranes cast with the thermal-inversion process suggest that the local pore size of a phase-separated polymer/solvent sys-

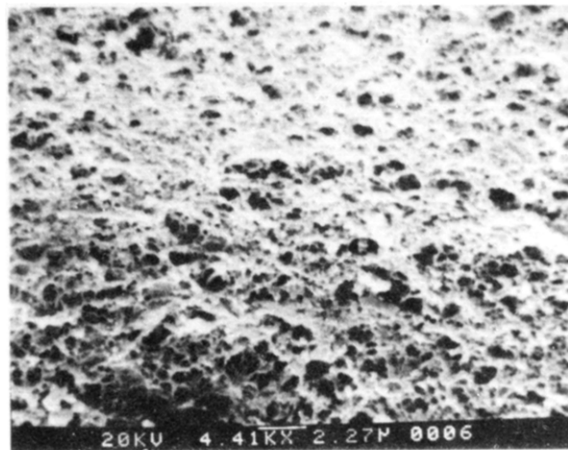


Figure 20. Scanning electron micrograph of the surface of a thermal-cast PMMA membrane in contact with the thermal insulator during coagulation. The starting solution is 15 wt % PMMA, and pore size is 1 μm . Scale bar corresponds to 2.27 μm .

tem decreases with decreasing coagulation temperature. Pores close to the cooling face form at a lower temperature than those in the interior or near the back surface. On the basis of arguments presented in the theory section, this trend implies that for a phase-separated system the absolute magnitude of the thermodynamic factor increases with decreasing temperature (Figure 7). For the particular polymer/solvent system, this is consistent with the fact that both species under study are highly polar. The energy of interaction between the polymer and solvent is large, producing a large enthalpic contribution to the χ -parameter.

The only difference between samples cast from the 10 and 15 wt % starting solutions is quantitative in nature. Two possible explanations exist. For a phase-separated system, the magnitude of the thermodynamic factor can be greater for average compositions of 15 wt % PMMA than for 10 wt % PMMA. If the induction times for structural growth are comparable for both starting polymer compositions, we can expect the pore sizes for a starting composition of 15 wt % PMMA to be smaller than those for 10 wt % PMMA. If the induction times for structural growth in the two solutions differ appreciably, a similar trend is obtained if induction times for a starting composition of 15 wt % PMMA are greater than those for 10 wt % PMMA. Even if the thermodynamic factors are essentially the same for both starting solutions, variations in induction times imply that at a given temperature the mobility factor for 10 wt % PMMA is greater than that for 15 wt % PMMA. The validity of this deduction can be examined through the self-diffusivities of the polymer segment and solvent at the particular temperature. The locations of relative maxima for the mobility vs. concentration curves (Figure 6) are roughly related to the relative ratios of the self-diffusivities of the polymer segment and solvent. If the self-diffusivity of the polymer segment is greater than that of the solvent, the maximum in the mobility vs. concentration curve at this particular temperature is shifted to low polymer concentrations. In realistic cases, it can be below 10 wt % polymer because sulfolane is a relatively viscous solvent at our casting temperatures. This means that above 0.10 polymer segment fraction, the mobility (and diffusivity) at a certain temperature decreases with polymer concentration. The consequence is a continuous reduction in pore sizes with polymer concentrations beyond this point. Pore sizes obtained from a starting solution of 15 wt % PMMA will thus be smaller than those for 10 wt % PMMA. Note that

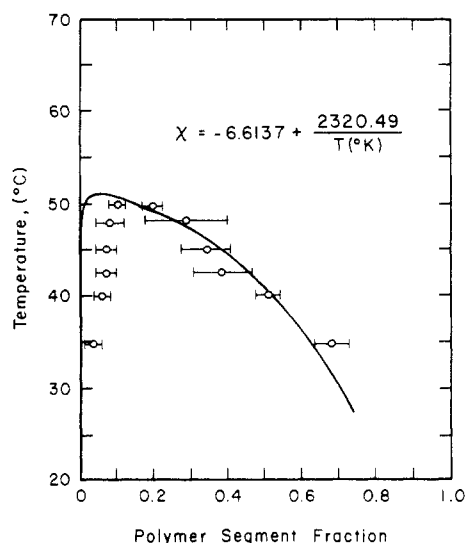


Figure 21. Binary phase diagram for a PMMA/sulfolane system. Data with error bars are obtained by pulsed-FTNMR techniques. The solid curve is calculated by using the Flory-Huggins theory with the χ -parameter shown in the figure.

growth of the phase-separated structure in the former starting solution occurs at lower temperatures than in the latter.

To understand the result obtained for the membrane cast from 5 wt % PMMA, we first refer to Figure 21, the binary phase diagram obtained with the use of pulsed-FTNMR techniques.¹⁹ For this polydisperse polymer sample, the phase diagram is not as broad as what could possibly be obtained by any reasonable set of parameters from the Flory-Huggins theory; i.e., the solvent-rich phase has more polymer in it, while the polymer-rich phase has less polymer. As shown with the solid curve, the thermodynamic theory cannot match experimental data, especially in the solvent-rich portion of the binodal curve. On the basis of this plot, if a dilute starting solution is used for thermal casting, the temperature near the face that is exposed to the cooling medium must be sufficiently lowered before phase separation ensues. Hence, a smaller range in temperature for phase separation in different parts of the sample exists than for a more concentrated starting solution. Different slices of the membrane cast from 5 wt % PMMA will therefore follow similar trajectories that all enter the phase-separated region at a temperature very close to its final values. This allows very little variation of pore sizes across the sample, and a uniform pore structure is obtained. Another possible explanation for obtaining an isotropic porous structure is that the system could have been confined to the metastable region during phase separation. This possibility exists because of the influence of short-chain components of the polymer in the overall phase behavior of the system. As Scott²⁰ pointed out, for a polydisperse polymer system, low molecular weight material actually makes the higher fractions more soluble. This statement can also explain our experimental observations on the rather peculiar shape of the binodal curve; i.e., more polymer can be found in the solvent-rich phase than for a monodisperse system. Thus, the solvent-rich side of the spinodal curve will also contain more polymer than that for a monodisperse system.

Koningsveld et al.²¹ concluded that the nonuniformity of local polymer segment concentration at high dilution can also affect the phase behavior of a polydisperse polymer system. These complications for a polydisperse system are difficult to accommodate in our modeling work. Effects

of this phenomenon are the broadening of both the binodal and spinodal curves for a polydisperse system. The present state of knowledge of phase behavior of polydisperse polymer systems is one of the reasons why our model invokes the Flory-Huggins theory instead of the more elaborate theories that also fail to quantify the effects of polydispersity.

Conclusion

We have demonstrated that anisotropic membranes can be obtained with a thermal inversion process. To optimize the process, polar polymer and solvent pairs are chosen. This condition is met by the PMMA/sulfolane system studied. A range of sample morphologies has been obtained with different starting concentrations. The 10% and 15% solutions both produce anisotropic membranes, whereas the 5% solution results in a porous membrane. The average pore size decreases with increasing starting solution concentration.

For a phase-separated system, the mutual diffusivity is negative inside the spinodal curve. This is due to the negative thermodynamic factor, while the mobility is always positive. With polar components, the absolute magnitude of the thermodynamic factor inside the spinodal increases rapidly with decreasing temperature. With spinodal decomposition, the final pore size increases with a decrease in the absolute magnitude of the thermodynamic factor. We have also shown that the growth of structure is an accelerated process; the induction time decreases with the mutual diffusivity at the average composition of the polymer/solvent system. When the phase-separation process is about 40% complete, a further decrease in temperature does not change the pore size established during the early stages of spinodal decomposition; i.e., the original structure has been locked in. Since the material close to the cooling medium is effectively phase-separated at a lower temperature than the material close to the thermal insulator, the final membrane pore size in the former is less than that in the latter.

Acknowledgment. This work was supported by the Polymer-Polymer Composites Program of the Center for Advanced Materials of Lawrence Berkeley Laboratory and the National Science Foundation through Grant CPE-8318681.

Registry No. PMMA (homopolymer), 9011-14-7.

References and Notes

- (1) Loeb, S.; Sourirajan, S. *Adv. Chem. Ser.* **1963**, No. 38, 117.
- (2) Tanny, G. B. *J. Appl. Polym. Sci.* **1974**, *18*, 2149.
- (3) Broens, L.; Altena, F. W.; Smolders, C. A.; Koenhen, D. M. *Desalination* **1980**, *32*, 33.
- (4) Strathmann, H.; Scheible, P.; Baker, R. W. *J. Polym. Sci.* **1971**, *15*, 811.
- (5) Castro, A. J. U.S. Patent 4 247 498, Jan 27, 1981.
- (6) Sakai, Y.; Tsukamoto, H.; Fujii, Y.; Tanzawa, H. "Formation of Poly(methyl methacrylate) Membranes Utilizing Stereocomplex Phenomenon", in "Ultrafiltration Membranes and Applications"; Cooper, A. R., Ed.; Plenum Press: New York, 1980; pp 99-107.
- (7) Porter, M. C. *Harnessing Theory Pract. Appl., World Filtr. Congr., 3rd*, 1982 1982, Vol II, 451-471.
- (8) Strathmann, H.; Kock, K. *Desalination* **1977**, *21*, 241.
- (9) Strathmann, H.; Kock, K.; Amar, P. *Desalination* **1975**, *16*, 179.
- (10) Matz, R. *Desalination* **1972**, *10*, 1.
- (11) Koenhen, D. M.; Mulder, M. H. V.; Smolders, C. A. *J. Appl. Polym. Sci.* **1977**, *21*, 199.
- (12) Vrentas, J. S.; Duda, J. L. *J. Polym. Sci., Polym. Phys. Ed.* **1977**, *15*, 403.
- (13) Vrentas, J. S.; Duda, J. L. *J. Polym. Sci., Polym. Phys. Ed.* **1977**, *15*, 417.
- (14) Vrentas, J. S.; Duda, J. L. *Macromolecules* **1976**, *9*, 785.

- (15) Vrentas, J. S.; Duda, J. L.; Ni, L.-W. *Macromolecules* 1983, 16, 261.
- (16) Huston, E. L.; Cahn, J. W.; Hilliard, J. E. *Acta Metall.* 1966, 14, 1053.
- (17) Flory, P. J. *J. Chem. Phys.* 1942, 10, 51.
- (18) Tompa, H. "Polymer Solutions"; Butterworths: London, 1956.
- (19) Caneba, G. T.; Soong, D. S. *Macromolecules*, in press.
- (20) Scott, R. L. *J. Chem. Phys.* 1945, 13, 178.
- (21) Koningsveld, R.; Stockmayer, W. H.; Kennedy, J. W.; Kleintjens, L. A. *Macromolecules* 1974, 7, 73.

Polymer Membrane Formation through the Thermal-Inversion Process. 2. Mathematical Modeling of Membrane Structure Formation

Gerard T. Caneba* and David S. Soong

*Department of Chemical Engineering, University of California, Berkeley, California 94720.
Received April 11, 1985*

ABSTRACT: Formation of anisotropic membranes by thermal inversion is simulated by a model developed here. Structured membranes are formed when a polymer/solvent film is thermally coagulated from one face while the opposite face is thermally insulated. Both kinetics and thermodynamics of liquid-liquid phase separation are included in the analysis. Only noncrystalline polymers are considered, and the composition of the starting polymer solution is close to the critical or Θ composition of the polymer/solvent system. Hence, spinodal decomposition is taken as the mechanism of phase separation. For a given point in the membrane cross section, the degree of phase separation is characterized by the deviation of the fluctuating concentration profile from the concentration of the starting polymer solution. The use of the Flory-Huggins model for solution thermodynamics and Cahn-Hilliard theory for spinodal decomposition leads to a one-dimensional fourth-order nonlinear partial differential equation that describes the phase-separation behavior induced by thermal inversion. Periodic boundary conditions are employed as well as infinitesimal sinusoidal perturbations for the initial condition. The solution scheme includes local linearization (from a previous time step) through Fourier transformation, followed by the application of the Euler method to solve the resulting set of ordinary differential equations for the frequency components of the concentration. With this mathematical model, a reasonable membrane pore size profile consistent with experimental observations is obtained.

Introduction

Broens et al.¹ classified structure formation in polymer membranes into three mechanisms: (a) liquid-liquid phase separation; (b) gelation; and (c) crystallization. Liquid-liquid phase separation involves either nucleation and growth² or spinodal decomposition.³ Gelation involves the formation of microcrystalline regions much smaller than the nuclei. This generally takes place at high polymer concentrations. At lower polymer concentrations (10%–20%), crystallites of sizes not much smaller than the size of the nuclei are formed. This latter type of crystallization results in the formation of lamellar or spherulitic domains.

In this work, we will only study noncrystalline systems. Thus, only liquid-liquid phase-separation processes will be considered for membrane formation. Both thermodynamics and kinetics govern this process. For the thermodynamic part of the analysis, any of a number of models such as Flory-Huggins theory,^{4,5} Flory-Prigogine theory,⁶⁻⁹ or even the more sophisticated thermodynamic theories of Patterson¹⁰ and Prausnitz¹¹⁻¹³ can be adopted. Since we are only concerned about qualitative explanations for the formation of pore structures in polymer membranes, Flory-Huggins theory was chosen and later proven adequate for our purposes. However, for quantitative predictions, it may be more appropriate to use one of the other thermodynamic theories.

The experimental work described in part 1 of this series of papers indicates that thermal casting produces open-pore anisotropic membranes with starting compositions

in the semidilute region. Such region is close to the critical composition of a binary phase diagram, where the size of the metastable region is small. This means that we need to only focus on spinodal decomposition rather than nucleation and growth as the process for phase separation.^{14,15} To model spinodal decomposition, the phenomenological theory formulated by Cahn and Hilliard¹⁶ will be used rather than other approaches involving stochastic¹⁷⁻²² and molecular dynamical^{23,24} formulations. Such an approach is theoretically and computationally more tractable, considering the existence of a variety of thermodynamic and transport models for polymer systems. The free-volume theory²⁵⁻²⁸ for the mass-transport aspect of the analysis will be used in conjunction with Cahn and Hilliard's theory for the system free energy. To solve the numerical problem posed by this phase-separation analysis, we will adopt a one-dimensional version of the approach developed by de Fontaine²⁹ for spinodal decomposition in metal alloys. Although the method involves certain assumptions on the constitutive relations of polymeric systems, it will be shown later that the results are qualitatively correct and useful for making further predictions on the effects of other thermodynamic and kinetic parameters on the morphology of thermally cast membranes. In addition, the entire model can be easily extended to multicomponent systems and to higher dimensional cases.

Model Strategy

Before embarking on detailed modeling, we will first give a brief review of the thermal casting procedure. Thermal casting (Figure 1) induces the formation of pore structures in a polymer membrane by the removal of heat instead of by using a nonsolvent as the coagulating agent. The simplest starting material here is a binary polymer solution

* Present address: Department of Chemistry and Chemical Engineering, Michigan Technological University, Houghton, MI 49931.